Microphase Separation in Thermosetting Blends of Epoxy Resin and Poly(ϵ-caprolactone)-*block*-Polystyrene Block Copolymers

Fanliang Meng, Zhiguang Xu, and Sixun Zheng*

Department of Polymer Science and Engineering, Shanghai Jiao Tong University, Shanghai 200240, P. R. China

Received October 19, 2007; Revised Manuscript Received December 19, 2007

ABSTRACT: The block copolymers, poly(ϵ-caprolactone)-*block*-polystyrene (PCL-*b*-PS) with the linear and star-shaped topological structures were synthesized *via* the combination of ring-opening polymerization (ROP) and atom transfer radical polymerization (ATRP). The two block copolymers with the identical block compositions were incorporated into epoxy to access the nanostructured thermosets. The microphase-separated morphologies in the systems were investigated by means of atomic force microscopy (AFM) and small-angle X-ray scattering (SAXS). It is identified that the epoxy thermosets can display the long-ranged ordered nanostructures depending on the concentration of the diblock copolymers. By considering the miscibility of the subchains of the block copolymers with epoxy after and before the curing reaction, it is judged that the formation of the nanostructures followed the mechanism of reaction-induced microphase separation. It is noted that the nanoscaled morphologies of the thermosets are quite dependent on the macromolecular topologies of the block copolymers. For the epoxy thermosets containing the linear PCL-*b*-PS diblock copolymer, the spherical PS nanophases were arranged into cubic (e.g., bcc, fcc, or simple cubic) lattice whereas the PS nanophases into lamellar lattice while the thermosets contain the tetra-armed PCL-*b*-PS block copolymer. The difference in nanostructures for the epoxy thermosets has been interpreted on the basis of the restriction of topological structures of the block copolymers on the formation of nanophases.

Introduction

The control over morphology of multicomponent thermosets is important for the improvement of properties of the materials.[1] It is recognized that the formation of nanostructures in thermosets can further optimize the inter-component interactions and thus the properties of materials were improved.[1,2] Recently, the concept of incorporating amphiphilic block copolymers into thermosets has widely been accepted to prepare the materials with ordered or disordered nanostructures.[2] Hillmyer et al.[2a,b] proposed a strategy of creating the nanostructures in thermosets using amphiphilic block copolymers *via* the mechanism of self-assembly. In the protocol, precursors of thermosets act as selective solvents of block copolymers and some self-organized structures such as lamellar, bicontinuous, cylindrical, and spherical structures can be accessed in the mixtures depending on fraction of block copolymers before the curing reaction. In this approach, the role of the curing reaction is to lock in the preformed self-organized nanostructures although it has been identified that the nanostructures could undergo some small changes with the occurrence of the curing reaction.[2a,b] More recently, it is identified that ordered and/or disordered nanostructures can be alternatively formed *via* the approach of reaction-induced microphase separation in thermosets.[3] In this approach, it is not required that the amphiphilic block copolymers are self-organized into nanostructures before curing reaction; all the subchains of block copolymers are miscible with precursors of thermosets and only a part of subchains of block copolymers are microphase-separated out upon curing. Mechanistically speaking, the formation of nanostructures *via* self-assembly is based on the equilibrium thermodynamics in the mixtures of precursors of thermosets and amphiphilic block copolymers, which is governed by the nature of precursors of thermosets and block copolymers. Nonetheless, the morphological control *via* the mechanism of reaction-induced microphase separation is quite dependent on the competitive kinetics between polymerization and microphase separation. Compared to reaction-induced phase separation in the blends of thermoset and homopolymers or random copolymers, reaction-induced microphase separation of block copolymers in the thermosets occur in a confined fashion and on the nanometer scale owing to the presence of miscible blocks. However, this technique has not been deeply investigated vis-à-vis the self-assembly approach.

During the past few years, a variety of block copolymer architectures have been employed to access ordered (or disordered) nanostructures in thermosets. With the synthesis of versatile block copolymers,[5] one can have tremendous space for maneuvering to control the formation of nanostructures. In ample literature, the formation of ordered and disordered nanostructures was reported by incorporating AB type amphiphilic diblock (and/or ABA type triblock) copolymers into thermosets.[2,3] Nonetheless, the structural effect of block copolymers on the formation of nanostructures in thermosets was occasionally considered. Rebizant et al. [2j,2l] investigated the ordered nanostructures in epoxy thermosets containing ABC triblock copolymers, e.g., polystyrene-*block*-polybutadiene-*block*-poly(methyl methacrylate). In this system, the poly(methyl methacrylate) subchain in the block copolymers remains miscible with epoxy thermosets after and before curing reaction. Serrano et al.[3d,3e] reported the formation of the ordered nanostructures in epoxy thermosets while the star-shaped block copolymers (i.e., epoxidized polystyrene-*block*-polybutadiene-*block*-polystyrene) were employed. The epoxided polybutadine blocks participated in the formation of cross-linked networks of epoxy resin.

The purpose of this work is to investigate the formation of ordered nanostructures in the epoxy thermosets containing poly-

* To whom correspondence should be addressed. E-mail: szheng@sjtu.edu.cn. Telephone: 86-21-54743278. Fax: 86-21-54741297.

10.1021/ma7023232 CCC: $40.75
Published on Web 02/02/2008

(ϵ-caprolactone)-*block*-polystyrene (PCL-*b*-PS) block copolymers and the effects of star-shaped topology of block copolymers on ordered nanostructures. To this end, amphiphilic block copolymers, poly(ϵ-caprolactone)-*block*-polystyrene (PCL-*b*-PS) with the linear and star-shaped topologies were synthesized with the combination of ring-opening polymerization (ROP) and atomic transfer radical polymerization (ATRP). The design of the diblock copolymers is based on the knowledge that PCL is miscible with epoxy thermosets[6] after and before curing reaction whereas PS will undergo reaction-induced phase separation in its blends with epoxy resin.[3e] It is expected that the nanostructured epoxy thermosets can be prepared *via* reaction-induced microphase separation in this system. In this work, atomic force microscopy (AFM) and small-angle X-ray scattering (SAXS) are used to examine the ordered nanostructures formed *via* the reaction-induced microphase separation. The difference in nanostructures for the epoxy thermosets has been addressed on the basis of the restriction of topological structure of block copolymers on the formation of nanophases.

Experimental Section

Materials. Diglycidyl ether of bisphenol A (DGEBA) with the epoxide equivalent weight of 185∼210 was purchased from Shanghai Resin Co., China. 4,4′-Methylenebis (2-chloroaniline) (MOCA), benzyl alcohol, styrene, and copper(I) bromide were of analytically pure grade, obtained from Shanghai Reagent Co., China. ϵ-Caprolactone (CL) (99%) was purchased from Fluka Co. Germany. Before use, it was distilled over calcium hydride (CaH_2) under reduced pressure. Stannous octanoate [$Sn(Oct)_2$] was purchased from Aldrich Co. Prior to use, styrene was washed with 5% aqueous NaOH and deionized water, respectively, for three times and then was distilled over CaH_2 under reduced pressure. Pentaerythritol was sublimated under reduced pressure. *N*,*N*,*N*′,*N*″,*N*‴-pentamethyldiethylenetriamine (PMDETA) (Aldrich, 99%), 2-bromoisobutyl bromide (Aldrich, 97%) were used as received. Copper(I) bromide was purified according to the literature procedure.[4] Before use, toluene and tetrahydrofuran (THF) were dried by refluxing over sodium and by subsequent distillation.

Synthesis of Monohydroxyl-Terminated Poly(ϵ-caprolactone) (PCL-OH). Monohydroxyl-terminated poly(ϵ-caprolactone) (PCL-OH) was synthesized *via* the ring-opening polymerization (ROP) of ϵ-CL with benzyl alcohol as the initiator and $Sn(Oct)_2$ was used as the catalyst. Typically, benzyl alcohol (0.3643 g, 3.37 mmol) and ϵ-CL (20.0000 g, 175.4 mmol) were charged to a 100 mL round-bottom flask equipped with a dry magnetic stirring bar and $Sn(Oct)_2$ (1/1000 wt with respect to ϵ-CL) was added using a syringe. The flask was connected to a standard Schlenk line and the reactive mixture was degassed *via* three pump−freeze−thaw cycles and then immersed in a thermostated oil bath at 120 °C for 24 h. The crude product was dissolved in tetrahydrofuran and the solution was dropped into an excessive amount of petroleum ether to afford the procipitates. This procedure was repeated three times to obtain white solids with the yield of 96%. The molecular weight of PCL-OH was estimated by means of ^{1}H NMR spectroscopy. The molecular weight of the PCL-OH was calculated to be M_n = 5700 according to the ratio of integration intensity of aliphatic methylene protons to aromatic protons.

Synthesis of Tetraarmed Star-Shaped Poly(ϵ-caprolactone). The tetraarmed star-shaped poly(ϵ-caprolactone) (*s*-PCL-OH) was synthesized *via* the ring-opening polymerization (ROP) of ϵ-CL with pentaerythritol as the initiator and $Sn(Oct)_2$ was used as the catalyst. Typically, pentaerythritol (0.1702 g, 1.25 mmol) and ϵ-CL (30.0300 g, 263.42 mmol) were charged to a 100 mL round-bottom flask equipped with a dry magnetic stirring bar. The flask was connected to a standard Schlenk line and the system was degassed *via* three pump−freeze−thaw cycles, and then the flask was put into an oil bath at 110 °C with vigorous stirring and $Sn(Oct)_2$ (1/1000 wt with respect to ϵ-CL) was added using a syringe. The pump−freeze−thaw process was carried out again and then the flask was immersed in a thermostated oil bath at 120 °C for 24 h. The crude product was dissolved in tetrahydrofuran, and the solution was dropped into an excessive amount of petroleum ether to afford the procipitates and this procedure was repeated three times to obtain white solids with a yield of 94.7%. The molecular weight of the PCL-OH was measured by means of gel permeation chromatography (GPC) to be M_n = 21 800 and M_w/M_n = 1.23, which is in a good agreement with the value of M_n = 22 720 calculated according to the ratio of integration intensity of terminal hydroxymethylene proton of PCL protons to pentaerythritol moiety protons.

Synthesis of *l*-PCL-*b*-PS Diblock Copolymer. In order to synthesize the linear poly(ϵ-caprolactone)-*block*-polystyrene (*l*-PCL-*b*-PS) diblock copolymer by means of atomic transfer radical polymerization (ATRP), the linear poly(ϵ-caprolactone) macroinitiator was first prepared by following the literature method.[3e] The above monohydroxyl-terminated PCL (*l*-PCL-OH) was employed to react with 2-bromoisobutyryl bromide in the presence of triethylamine, to afford the 2-bromoisobutyryl-terminated PCL [PCL-OOCCBr$(CH_3)_2$]. The linear poly(ϵ-caprolactone)-*block*-polystyrene (*l*-PCL-*b*-PS) diblock copolymer was synthesized by means of atom transfer radical polymerization (ATRP) from the PCL macroinitiator. In a typical experiment, PCL macroinitiator (5.0000 g, 0.862 mmol), Cu^{I}Br (0.1237 g, 0.862 mmol), PMDETA (180 μL, 0.862 mmol), and styrene (10.4 g, 96.2 mmol) were charged to a 100 mL round-bottom flask. The system was connected to the Schlenk line system and three freeze−pump−thaw cycles were used to remove the trace of moisture and oxygen. The reactive system was immersed into an oil bath at 110 °C for 12 h. The crude product was dissolved in tetrahydrofuran and passed through a neutral alumina column to remove the catalyst; the polymer solution was concentrated and then dropped into an excessive amount of cold methanol. The *l*-PCL-*b*-PS diblock copolymer was dried *in vacuo* at 40 °C for 48 h. The polymer (8.4700 g) was obtained with the controlled conversion of styrene monomer being 55%. The molecular weight of the block copolymer was determined by means of gel permeation chromatography (GPC) to be M_n = 14 100 with M_w/M_n = 1.12. In view of the length of PCL subchain in the block copolymer, the length of PS subchain of the block copolymer is calculated to be M_n = 8000.

Synthesis of Star Poly(ϵ-caprolactone)-*block*-polystyrene Diblock Copolymer. The tetra-armed diblock copolymer (*s*-PCL-*b*-PS) was obtained through the ATRP of styrene with the tetra-armed one as macroinitiator, i.e., *s*-PCL-OOCCBr$(CH_3)_2$. The star-shaped macroinitiator [*s*-PCL-OOCCBr$(CH_3)_2$] was obtained by the capping reaction of the tetra-armed PCL [*s*-PCL-OH] with 2-bromoisobutyryl bromide.[3e] Typically, the tetra-armed PCL [*s*-PCL-OH] (5.0000 g, 0.219 mmol), Cu^{I}Br (0.1258 g, 0.877 mmol), PMDETA (183 μL, 0.877 mmol), styrene (8.8700 g, 77.4 mmol) and 8 mL of anisole were charged to a 100 mL round-bottom flask. The flask was then connected to a standard Schlenk line, where a freeze−pump−thaw process was repeated for three times and then placed into an oil bath at 90 °C for 8 h. The crude product was dissolved in tetrahydrofuran and passed through a neutral alumina column to remove the catalyst; the polymer solution was concentrated and dropped into an excessive amount of cold methanol. The *s*-PCL-*b*-PS block copolymer was dried *in vacuo* at 40 °C for 48 h. The polymer (11.5 g) was obtained with the controlled conversion of styrene monomer being 83%. The molecular weight of the block copolymer was determined by means of gel permeation chromatography (GPC) to be M_n = 52 000 with M_w/M_n = 1.21. In view of the molecular weight of the star-shaped PCL, the length of PS subchain of the block copolymer is calculated to be M_n = 8200.

Preparation of Epoxy Thermosets Containing Block Copolymers. The block copolymers (i.e., *l*-PCL-*b*-PS and/or *s*-PCL-*b*-PS) were added to DGEBA and the mixtures were vigorously stirred at elevated temperature until the mixtures were homogeneous. Then equimolar MOCA with respect to the epoxide equivalence of DGEBA (the weight ratio of MOCA to DGEBA being 0.37:1) was added to the mixtures with vigorous stirring until homogeneous solutions were obtained again. The ternary mixture was poured into

Teflon molds and cured at 150 °C for 2 h plus 180 °C for 2 h for post curing.

Measurement and Characterization

Nuclear Magnetic Resonance Spectroscopy (NMR). The samples were dissolved in deuteronated chloroform and the NMR spectra were measured on a Varian Mercury Plus 400 MHz NMR spectrometer with tetramethylsilane (TMS) as the internal reference.

Gel Permeation Chromatography (GPC). The molecular weights and molecular weight distribution of polymers were determined on Waters 717 Plus autosampler gel permeation chromatography apparatus equipped with Waters RH columns and a Dawn Eos (Wyatt Technology) multiangle laser light scattering detector and the measurements were carried out at 25 °C with tetrahydrofuran (THF) at the elution rate of 1.0 mL/min.

Atomic Force Microscopy (AFM). The specimens of thermosets for AFM observation were trimmed using a microtome machine and the thickness of the specimens is about 70 nm. The morphological observation of the samples was conducted on a Nanoscope IIIa scanning probe microscope (Digital Instruments, Santa Barbara, CA) in tapping mode. A tip fabricated from silicon (125 μm in length with *ca.* 500 kHz resonant frequency) was used for scan, and the scan rate was 2.0 Hz.

Small-Angle X-ray Scattering (SAXS). The SAXS measurements were taken on a Bruker Nanostar system, Germany. Two-dimensional diffraction patterns were recorded using an image intensified CCD detector. The experiments were carried out at room temperature (25 °C) using Cu Kα radiation (λ = 1.54 Å, wavelength) operating at 40 kV, 35 mA. The intensity profiles were output as the plot of scattering intensity (I) vs scattering vector, $q = (4/\lambda) \sin(\theta/2)$ (θ = scattering angle).

Scanning Electron Microscopy (SEM). In order to observe the phase structure of epoxy blends, the thermosets were fractured under cryogenic condition using liquid nitrogen. The fractured surfaces so obtained were immersed in THF at room temperature for 30 min. The macroscopically separated phases (if any) can be preferentially etched by the solvent while epoxy matrix phase remains unaffected. The etched specimens were dried to remove the solvents. The fracture surfaces were coated with thin layers of gold of about 100 Å. The thermosets containing *s*-PCL-*b*-PS were examined with a JEOL JSM 7401F field emission scanning electron microscope (FESEM) at an activation voltage of 5 kV.

Fourier Transform Infrared Spectroscopy (FTIR). The FTIR was measured by a Perkin-Elmer Paragon 1000 Fourier transform spectrometer. The block copolymer was dissolved in THF and then the solution was cast onto KBr windows. The solvent was evaporated in vacuo at 60 °C to obtain the specimen of films. For the samples of thermosets, the powder was mixed with KBr pellets to press into small flakes. All the specimens were sufficiently thin to be within a range where the Beer−Lambert law is obeyed. In all cases 64 scans at a resolution of 2 cm^{-1} were used to record the spectra.

Differential Scanning Calorimetry (DSC). The calorimetric measurements were performed on a Perkin-Elmer Pyris 1 differential scanning calorimeter in a dry nitrogen atmosphere. The indium standard was used for temperature and enthalpy calibrations. The samples (about 8.0 mg in weight) were first heated to 180 °C and held at this temperature for 3 min to remove the thermal history, followed by quenching to −60 °C. A heating rate of 20 °C/min was used at all cases. The glass transition temperature (T_g) was taken as the midpoint of the heat capacity change. The melting temperatures (T_m's) were taken as the temperatures of the maximum of endothermic peak.

Results

Synthesis of Poly(ϵ-caprolactone)-*block*-polystyrene Diblock Copolymers. The synthetic routes of the block copolymers are shown in Scheme 1. The linear poly(ϵ-caprolactone)-*block*-polystyrene diblock copolymer (*l*-PCL-*b*-PS) was synthesized *via* the combination of ring-opening polymerization (ROP) and atom transfer radical polymerization (ATRP). In the first step, the ROP of ϵ-caprolactone (CL) was initiated with benzyl alcohol and with stannous octanoate [$Sn(Oct)_2$] as the catalyst to obtain the monohydroxyl-terminated poly(ϵ-caprolactone) (*l*-PCL-OH) with the desired molecular weight. The ^{1}H NMR spectroscopy was used to estimate the molecular weight of the *l*-PCL-OH and the molecular weight of the *l*-PCL-OH was calculated to be M_n = 5700 according to the ratio of the integration intensity of protons in caprolactone moiety to that of aromatic protons in benzyl alcohol in the ^{1}H NMR spectrum. The *l*-PCL-OH was used further to react with methyl 2-bromopropionate in the presence of triethylamine to prepare 2-bromoisobutyryl-terminated PCL, which was used as the macroinitiator to afford the linear poly(ϵ-caprolactone)-*block*-polystyrene diblock copolymer (*l*-PCL-*b*-PS) *via* the atom transfer radical polymerization (ATRP) of styrene. The ^{1}H NMR spectroscopy shows that this polymer combined the structural features from PCL and PS chains. In terms of the ratio of the integration intensities of styrene moiety protons to those of methylene (−CH_2−) protons in benzyl alcohol in the ^{1}H NMR spectrum, the length of the PS block and the molecular weight of the diblock copolymer were calculated to be $M_n \approx 8000$ and $M_n \approx 13\,700$, respectively. The diblock copolymer was further subjected to the measurement of gel permeation chromatography (GPC) and the GPC curve of the linear PCL-*b*-PS diblock copolymer was presented in Figure 1. The diblock copolymer displayed the feature of unimodal distribution of molecular

Scheme 1. Synthesis of *l*-PCL-*b*-PS and *s*-PCL-*b*-PS Block Copolymers

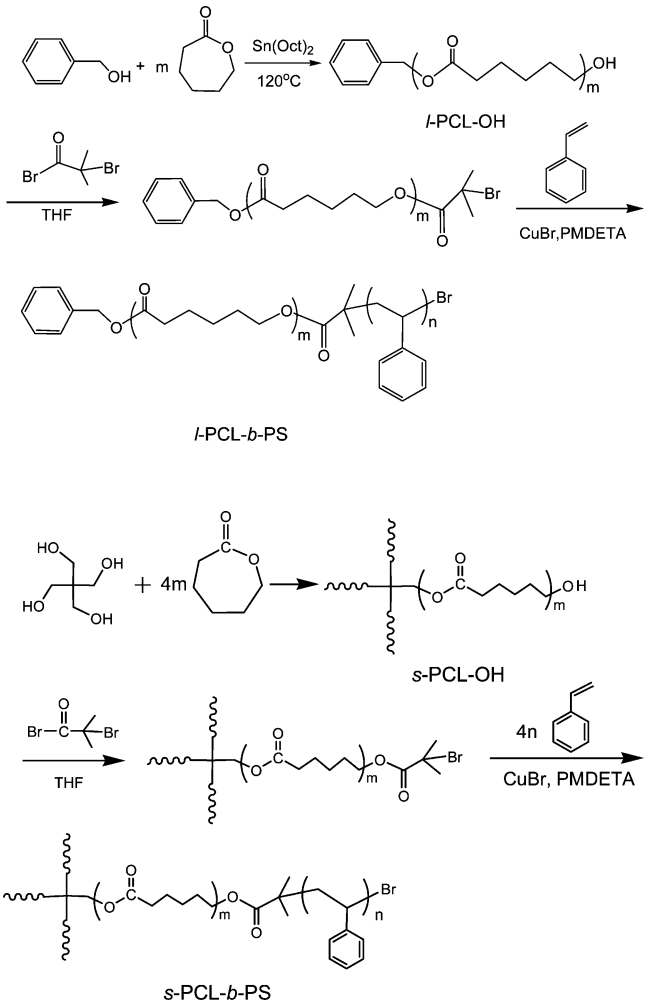

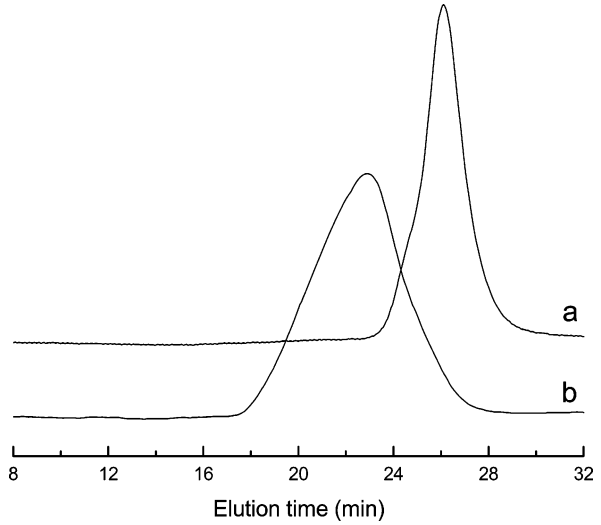

Figure 1. GPC curves of block copolymers: (a) linear diblock copolymer *l*-PCL-*b*-PS; (b) star-shaped diblock copolymer *s*-PCL-*b*-PS.

weight with the polydispersity of $M_w/M_n = 1.12$, implying that polymerizations are indeed in living fashions. The GPC results show that the diblock copolymer possesses the number-average molecular weight of $M_n = 14\,100$, which is in accordance with that of ^{1}H NMR spectroscopy.

The tetra-armed star-shaped block copolymer (*s*-PCL-*b*-PS) was also synthesized by the combination of ROP and ATRP. In the present work, pentaerythritol was used as the initiator to afford the tetra-armed star-shaped poly(ϵ-caprolactone) (*s*-PCL-OH) *via* ROP of ϵ-caprolactone. The terminal hydroxyl groups of the star-shaped PCL were capped with 2-bromoisobutylryl bromide in the presence of triethylamine, in order to carry out the atom transfer radical polymerization of styrene as depicted in Scheme 1. In views of the ratio of the integration intensities of the protons from PS and PCL moieties to that of methylene ($-CH_2-$) in pentaerythritol protons in the ^{1}H NMR spectrum of the product, the molecular weight of the tetra-armed block copolymer was calculated to be $M_n = 54\,600$ and the lengths of PCL and PS subchains for the tetra-armed block copolymer was estimated to be $M_n = 5450$ and $M_n = 8200$, respectively. The curve of GPC of the polymer is also presented in Figure 1. The unimodal peak indicates that the block copolymer was obtained and the molecular weight of the tetra-armed star-shaped poly(ϵ-caprolactone)-*block*-polystyrene (*s*-PCL-*b*-PS) was measured to be $M_n = 52\,000$ with the polydispersity of $M_w/M_n = 1.21$. This result is in good agreement with those of ^{1}H NMR spectroscopy and the calculation according to the feed ratios and conversions of the monomers. It is noted that the polydispersity of *s*-PCL-*b*-PS ($M_w/M_n = 1.21$) is slightly higher than that of *l*-PCL-*b*-PS ($M_w/M_n = 1.12$).

Shown in Figure 2 are the DSC curves of the above PCL-*b*-PS block copolymers. In the DSC thermograms, the glass transition of PS subchain appeared at about 72 °C, which is higher than the melting temperature of the PCL subchain. This observation suggests that the diblock copolymers are microphase-separated. It is noted that with the identical lengths of PCL subchains, the melting temperature (T_m) and melting enthalphy (ΔH_m) of PCL subchain in *s*-PCL-*b*-PS are significantly lower than those in *l*-PCL-*b*-PS. This phenomenon could be attributable to the confinement of star-shaped topology of *s*-PCL-*b*-PS diblock copolymer on the crystallization of PCL chain.[7]

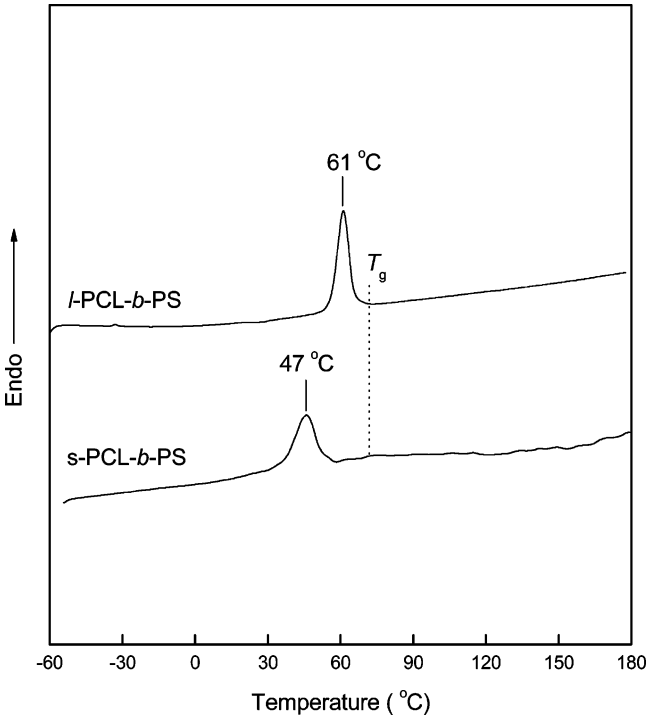

Figure 2. DSC curves of *s*-PCL-*b*-PS and *s*-PCL-*b*-PS.

Morphology of Epoxy Thermosets containing PCL-*b*-PS Block Copolymers. The PCL-*b*-PS block copolymers were incorporated into epoxy to prepare the nanostructured thermosets. Before the curing reaction, all the ternary mixtures composed of DGEBA, the curing agent (i.e., MOCA), and the PCL-*b*-PS block copolymers were homogeneous and transparent, suggesting that no macroscopic phase separation occurred at the scale exceeding the wavelength of visible light at room and curing temperatures. The mixtures were cured at 150 °C for 2 h plus 180 °C for 2 h and the epoxy thermosets were obtained with the content of PCL-*b*-PS block copolymers up to 40 wt %. All the thermosets are homogeneous and transparent, implying that macroscopic phase separation did not take place with the occurrence of curing reaction. The cured thermosets were trimmed using an ultrathin microtome and the sections were subjected to the morphological observations by means of atomic force microscopy (AFM).

The AFM images of the thermosets containing 10, 20, 30, and 40 wt % of *l*-PCL-*b*-PS diblock copolymer are presented in Figure 3. The left and right images are the topography and phase contrast images, respectively. In terms of the volume fraction of PS and the difference in viscoelastic properties between epoxy matrix and PS phases, the light continuous regions are assignable to the cross-linked epoxy matrix, which were interpenetrated by the PCL blocks of the copolymer while the dark regions are attributed to PS domains. It is seen that all the thermosets exhibited microphase-separated morphologies. It is observed that for the thermoset containing 10 wt % of diblock copolymer the nanoscaled PS spherical particles with the size of 10−20 nm were homogenously dispersed in the continuous epoxy matrix. With increasing the content of the diblock copolymer, some interconnected PS microdomains began to appear (Figure 3b) and the quantity of the PS microdomains was increased whereas the size of the spherical particle remains almost invariant (Figure 3a,b). When the concentration of diblock copolymer is 30 wt % or more, the ordered nanostructures were identified even from bare eyes (Figure 3, parts c and d). The morphologies of the thermosetting

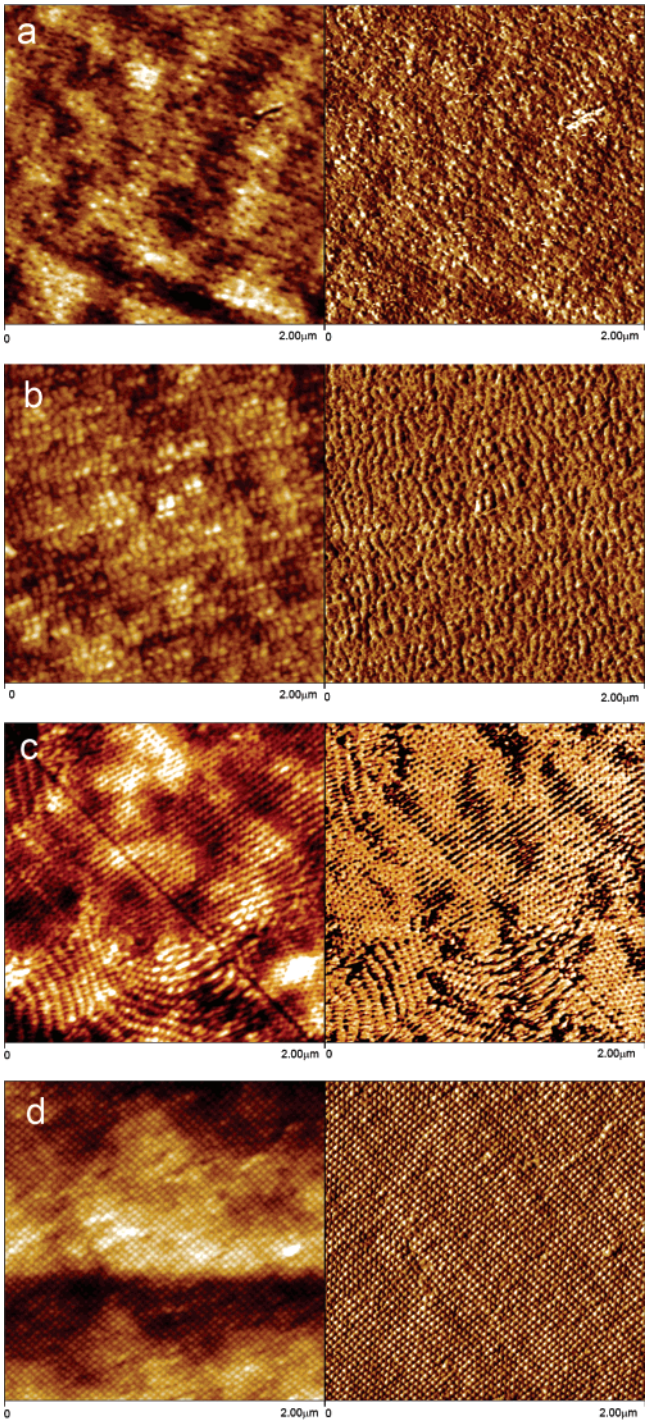

Figure 3. AFM images of the thermosets containing (a) 10, (b) 20, (c) 30, and (d) 40 wt % of linear *l*-PCL-*b*-PS diblock copolymer. Left: topography. Right: phase contrast images.

blends were further investigated by small-angle X-ray scattering (SAXS). The SAXS profiles of the thermosets containing 10, 20, 30, and 40 wt % of *l*-PCL-*b*-PS diblock copolymer are shown in Figure 4. It is seen that the well-defined scattering peaks were observed in all the cases, indicating that the thermosets containing *l*-PCL-*b*-PS are microphase-separated. In addition, it is noted that, except for the thermoset containing 10 wt % of *l*-PCL-*b*-PS diblock copolymer, the epoxy thermosets displayed the multiple scattering maxima as denoted with the arrows, indicating that the epoxy thermosets possess long-range ordered nanostructures. The positions of the scattering maxima remain essentially constant, apart from some slight shifts to the higher q values with increasing the content of *l*-PCL-

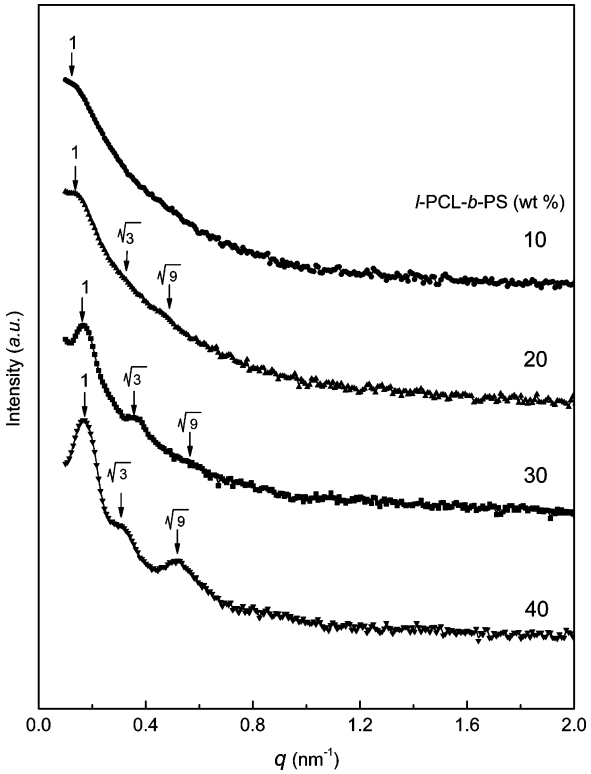

Figure 4. SAXS profiles of the thermosets containing linear *l*-PCL-*b*-PS diblock copolymer. Each profile has been shifted vertically for clarity.

b-PS. According to the position of the primary scattering peaks, the principal domain spacing d_m can be obtained to be 49.0, 45.2, 37.5, and 35.3 nm for the thermosets containing 10, 20, 30, and 40 wt % of *l*-PCL-*b*-PS diblock copolymer, respectively. This result is in a good agreement with those obtained by means of AFM. It is noted that the average distance between neighboring domains decreased with increasing the content of the diblock copolymer. The slight shifts of the scattering maxima could be associated with local rearrangement leading to an enhancement of the long-range order. The scattering peaks of the thermosets situated at q values of 1, $3^{0.5}$ and $9^{0.5}$ relative to the first-order scattering peak positions (q_m) are discernible. It is plausible to propose that these are the lattice scattering peaks of spherical (or cylindrical) nanophases arranged in cubic lattices such as body-centered cubic (bcc), face-centered cubic (fcc) or simple cubic symmetries. In addition, hexagonally packed cylindrical morphology is also possible. It should be pointed out that it is not easy unambiguously to judge the types of packing lattices only in terms of SAXS profiles for the thermosetting blends containing 20, 30 wt % *l*-PCL-*b*-PS since the scattering peaks are quite broad, i.e., the ordering is apparently not good enough.

The AFM micrographs of the epoxy thermosets containing 10, 20, 30, and 40 wt % of *s*-PCL-*b*-PS block copolymer are presented in Figure 5. It is seen that all the samples exhibited the nanostructured morphologies. For the thermoset containing 10 wt % of *s*-PCL-*b*-PS block copolymer, the PS microphases with irregular forms were dispersed in the continuous epoxy matrix with the size of 10 ∼ 20 nm (see Figure 5a). When the concentration of the diblock copolymer is more than 10 wt %, the PS domains increasingly became interconnected and a variety of worm-like nanoobjects were observed (Figure 5b,c). While the concentration of diblock copolymer is 40 wt % or more, the lamellar nanostructures were exhibited (Figure 5d). It is of interest to note that at the same concentration of block copolymer, the nanostructures of the thermosets containing

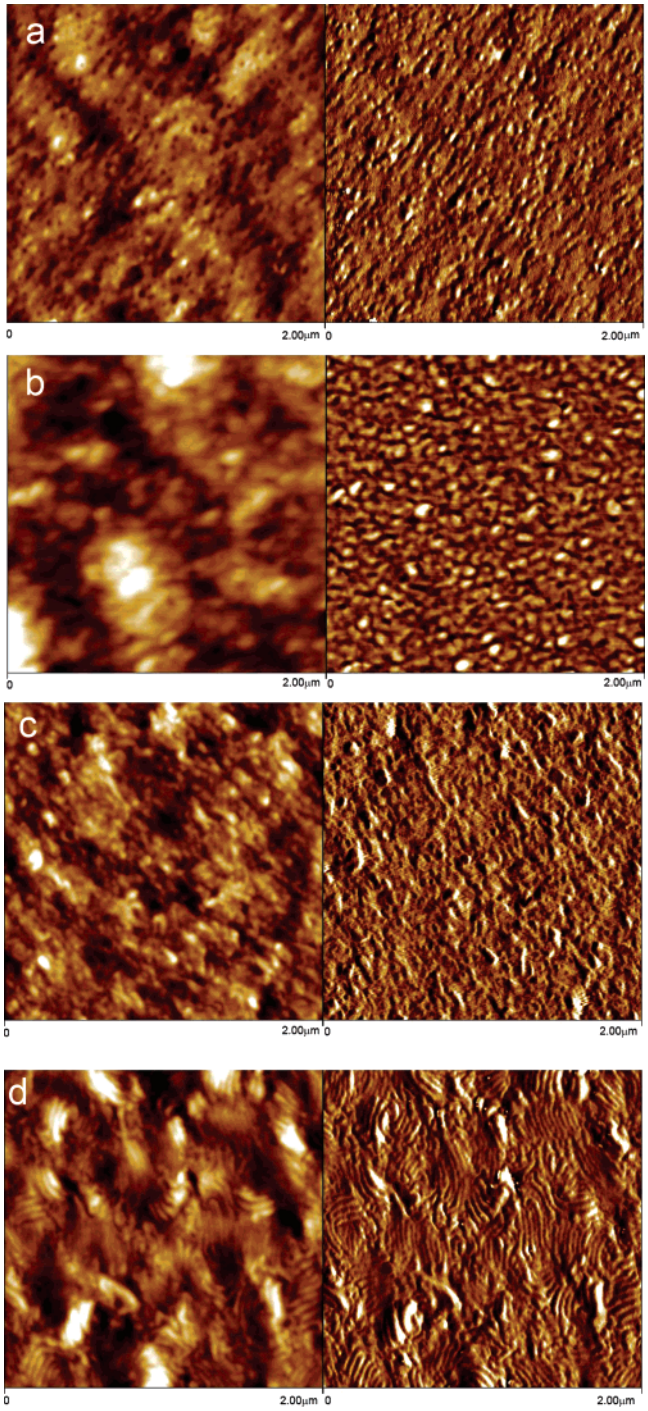

Figure 5. AFM images of the thermosets containing (a) 10, (b) 20, (c) 30, and (d) 40 wt % of *s*-PCL-*b*-PS diblock copolymer. Left: topography. Right: phase contrast images.

s-PCL-*b*-PS became less ordered than those of the thermosets containing *l*-PCL-*b*-PS. The nanostructures of the thermosets containing *s*-PCL-*b*-PS were further investigated by means of SAXS. Shown in Figure 6 are the SAXS profiles of the epoxy thermosets. All the SAXS profiles of thermosets displayed the primary scattering maxima in the vicinity of $q = 0.10$ nm^{-1}, indicating that all the epoxy thermosets containing *s*-PCL-*b*-PS are also microphase-separated. It is seen that the positions of the scattering maxima slightly shift to the higher q values with increasing the content of *s*-PCL-*b*-PS. According to the position of the primary scattering peaks, the principal domain spacing d_m can be obtained to be 67.4, 59.7, 49.7, and 46.6 nm for the thermosets containing 10, 20, 30, and 40 wt % of *s*-PCL-*b*-PS, respectively. It is noted that with the same content of diblock copolymers, the principal domain spacing d_m for the thermoset containing *s*-PCL-*b*-PS is significantly larger than that of the thermoset containing *l*-PCL-*b*-PS. The difference in d_m spacing could be related to the formation of different nanostructures between the two thermosetting nanocomposites. While the concentration of the diblock copolymer is 20 wt % or more, the multiple scattering maximum was also detected, implying that ordered nanostructures appeared in the thermosetting blends of epoxy with *s*-PCL-*b*-PS block copolymer. The scattering peaks of the thermosets are situated at the q values of 1, $4^{0.5}$, and $16^{0.5}$ relative to the first-order scattering peak positions (q_m) and these are the lattice scattering peaks of spherical (or cylindrical) nanophases arranged in lamellar lattices, which is in marked contrast to the epoxy thermosets containing *l*-PCL-*b*-PS.

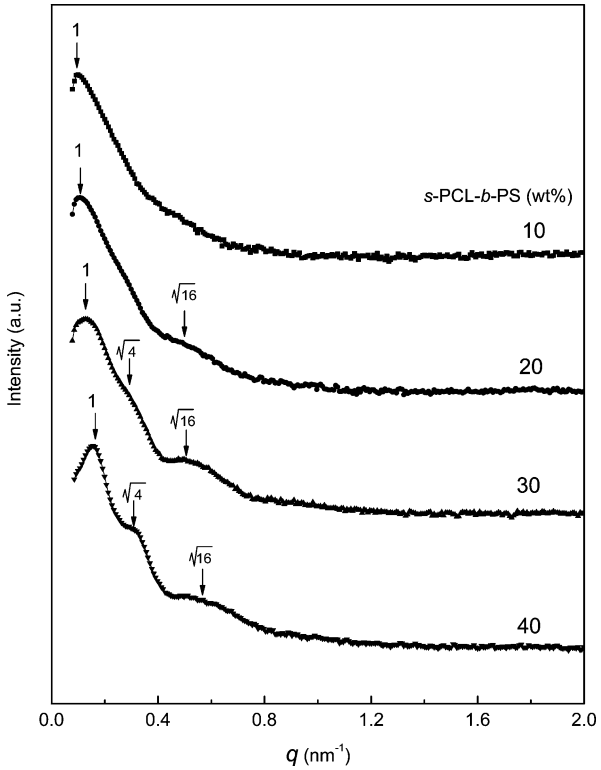

Figure 6. SAXS profiles of the thermosets containing *s*-PCL-*b*-PS diblock copolymer. Each profile has been shifted vertically for clarity.

Discussion

It has been identified that the formation of nanostructures in thermosets containing amphiphilic block copolymers could follow self-assembly[2] or reaction-induced microphase separation[3] mechanisms, depending on the miscibility of subchains of block copolymers with thermosets after and before curing reaction. Hillmyer et al.[2a,2b] proposed the strategy of creating nanostructures using amphiphilic block copolymers *via* self-assembly mechanism. In this protocol, the precursors of thermosets act as the selective solvents of block copolymers. Prior to curing reaction, the self-assembly microphases such as lamellar, bicontinuous, cylindrical, and spherical structures are formed in the mixtures depending on the blend composition. These nanostructures can be further fixed with introduction of hardeners and subsequent curing. With appropriate design of block copolymer architecture, the block copolymers self-assemble to form ordered or disordered nanostructures.[2] The prerequisite for the self-assembly approach is that block

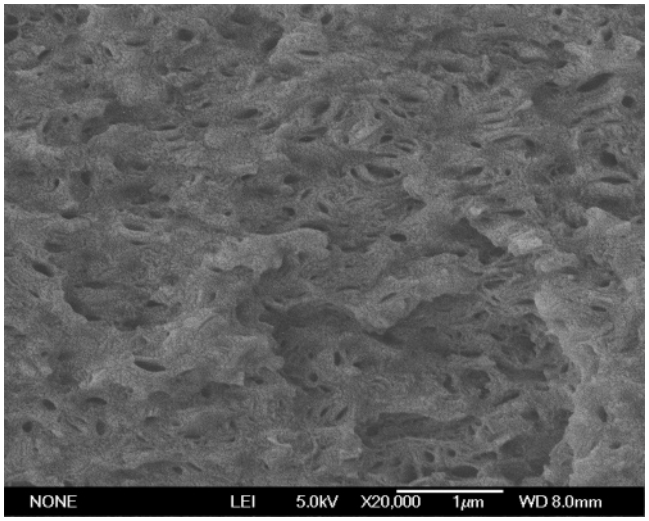

Figure 7. FESEM micrograph of the thermoset containing 40 wt % *s*-PCL-*b*-PS.

copolymers are self-organized into micelle (or vesicle) structures in their mixtures with precursors of thermosets prior to curing; the role of curing reaction is to lock in the morphology that is already present although it was identified that there were some small changes in the nanostructures after and before curing reaction.[2a,b] However, self-organization of amphiphilic block copolymers in the precursors of thermosets does not always occur. In many circumstances all the subchains of block copolymers are actually miscible with the precursors of thermosets. The miscibility (or solubility) is ascribed to the non-negligible entropic contribution (ΔS_m) to free energy of mixing (ΔG_m) in the mixtures of block copolymers since the precursors (or monomers) of thermosets are generally some compounds of low molecular weights.[1] In addition, the presence of the self-organized microphases formed at lower temperatures does not purport the survival of these structures at elevated temperatures that are required for curing of some high performance thermosets since the mixtures of polymers with precursors of thermosets generally displayed upper critical solution temperature (UCST) behaviors.[1] Under this circumstance, it is proposed that the nanostructured thermosets can be alternatively prepared *via* the approach of reaction-induced microphase separation. In this approach, all the blocks of copolymers are miscible with precursors of thermosets, i.e., no self-assembled nanostructures were formed before curing reaction. The nanostructures are only created *via* reaction-induced microphase separation of a part of blocks of amphiphilic copolymers whereas the other blocks remain miscible with the cross-linked matrix.

In the present case, the block copolymers (*viz.*, *l*-PCL-*b*-PS and *s*-PCL-*b*-PS) were exploited to access the nanostructures of epoxy thermosets. It has been known that PCL is miscible with epoxy after and before curing reaction[7] whereas the mixtures composed of PS and epoxy precursors displayed an upper critical solution temperature (UCST) behavior; the reaction-induced phase separation can occur when the curing reaction is carried out at the temperature above the critical solution temperature (e.g., 150 °C).[3g] Therefore, it is judged that in the present case the formation of nanostructures follows the reaction-induced microphase separation other than self-assembly mechanism.

In this work, the combination of two approaches of living polymerization (i.e., ROP and ATRP) was employed to prepare the PCL-*b*-PS block copolymers with the identical composition and thus the impact of the topologies of diblock copolymers (i.e., linear and star-shaped structures) on the nanostructures in the thermosets was examined. It is of interest to note that the nanophases in the epoxy thermosets containing *l*-PCL-*b*-PS were arranged into the ordered lattices such as body-centered cubic (bcc), face-centered cubic (fcc) or simple cubic lattices while the nanodomains in the thermosets containing *s*-PCL-*b*-PS can be packed into lamellar nanostructures. The fact that the less ordered nanostructures were formed in the epoxy thermosets containing *s*-PCL-*b*-PS could result from the confinement of the star-shaped topology of the block copolymer on the reaction-induced microphase. It is known that in the thermoset blends of epoxy resin with a homopolymer (or random copolymer), reaction-induced phase separation is governed by the competitive kinetics between polymerization and phase separation. The mechanism of spinodal decomposition (SD) (or/and nucleation and growth, NG) induced by polymerization results in the formation of very fine phase-separated structures at the micrometer scale.[1,2] While an amphiphilic block copolymer is used instead of the homopolymer (and/or random copolymer), phase separation occurs in a confined manner. In the present case, the PCL subchains of the diblock copolymers are miscible with epoxy matrix and thus the growth of PS domains will be confined to the nanometer scale. The macroscopic phase separation is thus suppressed by the presence of the PCL subchains, which depress the surface free energy of PS particles. For the epoxy thermosets containing *l*-PCL-*b*-PS diblock copolymer, it is noted that the size of the PS microdomains is quite uniform and the uniformly distributed PS microdomains were densely packed into the ordered nanostructures (e.g., long-rang ordered cubic lattice). In contrast to the epoxy thermosets containing *l*-PCL-*b*-PS, the less ordered nanostructures were obtained in the epoxy thermosets containing *s*-PCL-*b*-PS. It is plausible to propose that the morphological difference results from the effect of topological structures of PCL chains. For the epoxy thermosets containing *l*-PCL-*b*-PS diblock copolymer, the linear PCL subchains with single free ends are homogenously dispersed around the PS nanodomains, which effectively reduce the surface free energy of PS nanoparticles. In the case of the epoxy thermosets containing *s*-PCL-*b*-PS, every four PCL subchains were "wrapped" into a "nodule". Compared to its linear counterpart, the mixing entropy of the wrapped miscible PCL subchains in the epoxy matrix is significantly decreased, which would ineffectively reduce the surface energy of PS nanodomains. It is plausible to propose that the reduction in the surface energy of PS nanodomains is responsible for the formation of lamellar nanostructures. It should be pointed out that the difference in the morphologies of the epoxy thermosets containing different block copolymers with the identical composition could be also associated with some kinetic factors in addition to the above interpretation according to thermodynamics. Each arm of the *s*-PCL-*b*-PS block copolymer has the identical length and composition with *l*-PCL-*b*-PS. Therefore, the molecular weight of *s*-PCL-*b*-PS is four times as that of *l*-PCL-*b*-PS. The difference in molecular weights could exert some significant influence on viscosity, rheokinetics of microphase separation and viscoelasticity of microphase *etc.* in the *in situ* polymerization blending systems and thus the morphological structures of blends were affected. It should be pointed out that the formation of the lamellar nanostructure for the modification with 40 wt % *s*-PCL-*b*-PS is not attributed to the occurrence of phase inversion as evidenced by scanning electronic microscopy (SEM). Shown in Figure 7 is the micrograph of field emission scanning electronic microscopy

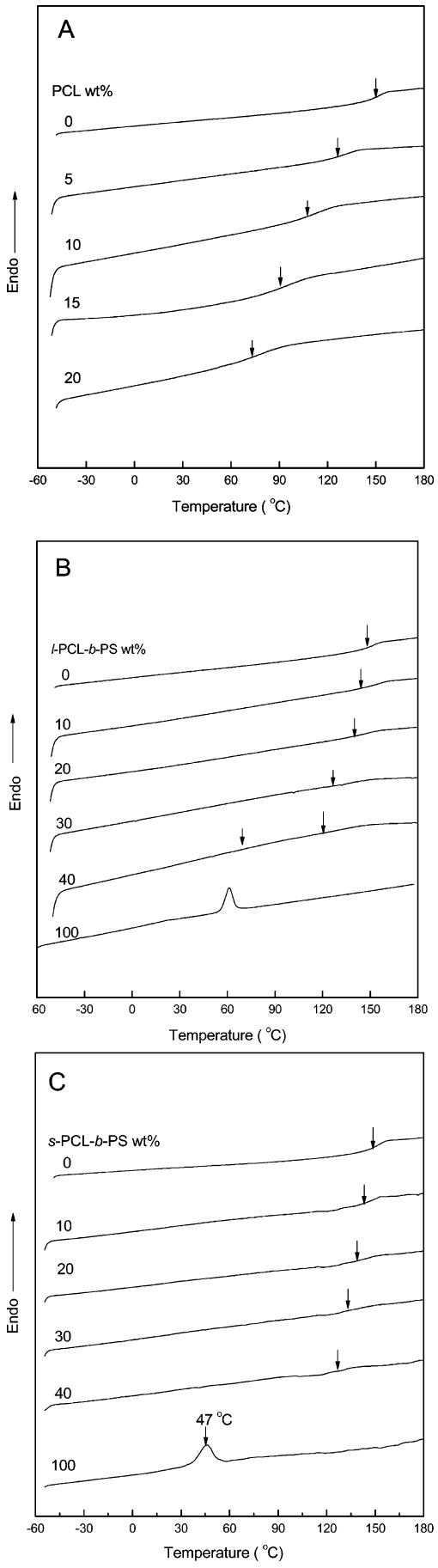

Figure 8. DSC curves of epoxy thermosets: (A) binary blends containing the model PCL; (B) nanostructured thermosets containing *l*-PCL-*b*-PS. (C) nanostructured thermosets containing *s*-PCL-*b*-PS.

(FESEM) for the thermoset containing 40 wt % *s*-PCL-*b*-PS. The lamellar nanostructure is discernible at the surface of the fracture end and no feature of phase inversion was exhibited. The morphology revealed by EFSEM is in good agreement with that by AFM.

The above effects could be taken as the restriction of star-shaped topology of the block copolymer on the formation of the ordered nanostructures, which could be readily reflected by the behavior of glass transition of the nanostructured thermosets. The nanostructured thermosets were subjected to thermal analysis and the DSC curves are shown in Figure 8. In the DSC thermogram of *l*-PCL-*b*-PS (and/or *s*-PCL-*b*-PS) a sharp endothermic peak at 61 °C (and/or 47 °C) was displayed, which is assignable to the melting transition of PCL subchain of the block copolymer. It is noted that all the thermosets investigated did not exhibit the melting transition of PCL subchains, suggesting that PCL subchains are not crystalline in the nanostructured thermosets. It is propose that the PCL subchains are miscible with the epoxy thermosets and are trapped into the cross-linked epoxy networks. The miscibility was further evidenced by the depression in glass transition temperatures (T_g's) for the epoxy-rich phases as shown in Figure 8. It is seen that each thermoset containing the diblock copolymers displayed single T_g, which decreased with increasing the concentration of the block copolymers. The decreased T_g's resulted from the plasticization of miscible PCL on epoxy matrix. It is noted that that at the same content of block copolymer the epoxy thermosets containing *s*-PCL-*b*-PS significantly exhibited the higher T_g's than the thermosets containing *l*-PCL-*b*-PS block copolymer. For comparison, the glass transition behavior of the binary thermosetting blends of epoxy and the model PCL with the identical molecular weight with the PCL subchains of the copolymers was also investigated by means of DSC. The appearance of single and composition-dependent glass transition temperatures is indicative of the full miscibility of epoxy with the PCL.[8] There are several theoretical and empirical equations to account for the dependence of glass transition temperature on blend composition.[9] Of them, the Couchman equation[9c] is frequently used:

$$\ln T_g = [W_1 k \ln T_{g1} + W_2 \ln T_{g2}]/(W_1 k + W_2) \qquad (1)$$

where W_i is the weight fraction of component i and T_g is the glass transition temperature of blend; the parameter k is the Couchman coefficient defined by

$$k = \Delta C_{p1}/\Delta C_{p2} \qquad (2)$$

where ΔC_{pi} designates the increment of the heat capacity of the specimen at glass transition. In the present work, the value of k was determined to be 1.68 for the binary blends of epoxy with the model PCL as shown in Figure 9. However, it is noted that at the same content of PCL chains, the T_g's of the nanostructured thermosets are significantly higher than those of the binary thermosetting blends of epoxy and PCL at the same compositions of epoxy and PCL. Furthermore, the thermosets containing *s*-PCL-*b*-PS diblock copolymer exhibited the higher T_g's than the thermosets containing *l*-PCL-*b*-PS with the identical content of PCL blocks. It is proposed that compared to the binary blends of epoxy with the model PCL the increased T_g's could be associated with the formation of the nanostructures in the thermosets. In the binary thermosetting blends, the PCL chains were homogeneously dispersed into the epoxy matrix and were well interpenetrated into the cross-linked epoxy networks *via* the formation of the intermolecular hydrogen

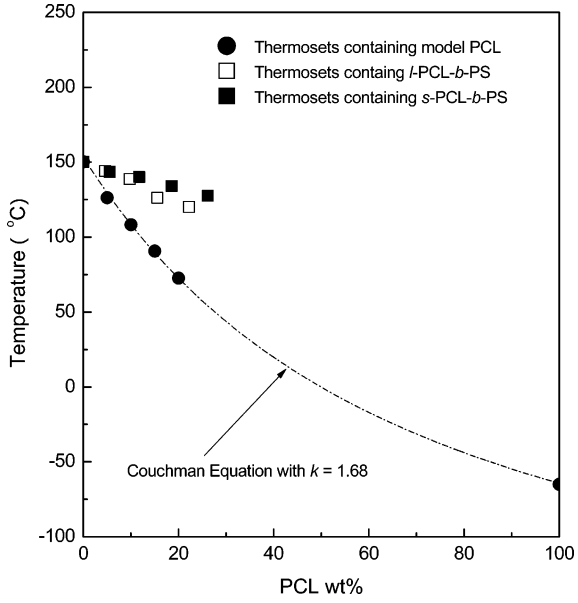

Figure 9. Plots of glass transition temperatures (T_g's) as functions of PCL content.

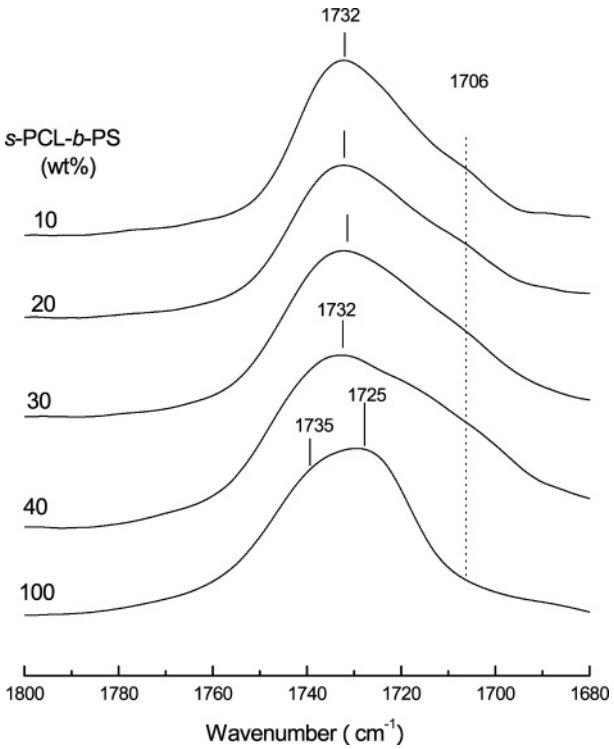

Figure 10. FTIR spectra of the nanostructured thermosets containing *s*-PCL-*b*-PS in the range of 1650−1800 cm^{-1}.

bonding interactions. In contrast, the PCL chains have to be enriched at the surface of the microphase-separated PS nanodomains due to the presence of chemical bonds between PS and PCL subchains in the composites. Because of the steric hindrance, the PCL chains at the intimate surface of PS nanodomains could not be well mixed with epoxy matrix and thus the less PCL chains were interpenetrated with the epoxy matrix in the nanocomposites, i.e., the plasticization of PCL chains on the epoxy matrix would be effectively weakened, which causes the increased T_g's of epoxy matrix. This effect has been reported in the self-assembly of epoxy resin and amphiphilic block copolymer nanocomposites.[2a,2b] Nonetheless, this effect is increasingly pronounced in the thermosets containing *s*-PCL-*b*-PS block copolymer due to the restriction of star-shaped topology on the mixing of PCL with the epoxy matrices. This result suggests that due to the presence of the star-shaped topology the PCL subchains in the thermosets containing *s*-PCL-*b*-PS cannot depress the surface free energy of PS domains as in the thermosets containing *l*-PCL-*b*-PS. This observation is helpful to interpret the cause of formation for the quite different nanostructures in the thermosets.

The miscibility of the PCL chains of the block copolymers with the cross-linked epoxy resin is ascribed to the formation of the intermolecular hydrogen bonding interactions, which is readily evidenced by Fourier transform infrared spectroscopy (FTIR). Representatively, the FTIR spectra of *s*-PCL-*b*-PS and the nanostructured thermosets containing *s*-PCL-*b*-PS in the range of 1660−1800 cm^{-1} are shown in Figure 10. The absorption bands are ascribed to the stretching vibration of carbonyl groups (>C═O) of PCL chains. At the room temperature, the carbonyl band of the pure block copolymers consists of two components sensitive to the conformation of PCL chains. The one component centered at 1735 cm^{-1} is characteristic of amorphous chains of PCL whereas the sharp band at 1725 cm^{-1} is ascribed to the carbonyls in the crystalline region of PCL. It is noted that in the FTIR spectra of the nanostructured thermosets, the bands of PCL crystals at 1725 cm^{-1} were absent, implying that the PCL chains exist in the thermosets in the amorphous state. Nonetheless, there appeared new shoulders at the lower frequency of 1706 cm^{-1} in the FTIR spectra of the nanostructured thermosets and the shoulder bands are assigned to the stretching vibration of hydrogen-bonded carbonyls,[10] i.e., there is the formation of the intermolecular hydrogen bonding interactions between the secondary hydroxyl groups of epoxy matrix and the carbonyl groups of PCL. In addition, the bands at 1735 cm^{-1} were found to shift to the lower frequency (1730 cm^{-1}) with increasing the concentration of the block copolymers. The FTIR results indicate that there existed the intermolecular hydrogen-bonding interactions between the PCL chains of the PCL subchains of the block copolymers and the epoxy networks.

Conclusions

The poly(ϵ-caprolactone)-*block*-polystyrene (PCL-*b*-PS) diblock copolymers with linear and star-shaped topological structures were synthesized *via* the combination of ring-opening polymerization (ROP) and atom transfer radical polymerization (ATRP). The two block copolymers with the identical compositions were incorporated into epoxy thermosets to access the nanostructures. The reaction-induced microphase separation in the systems was investigated by means of atomic force microscopy (AFM) and small-angle X-ray scattering (SAXS). Depending on the concentration of the diblock copolymers, the thermosets can display different long-ranged ordered nanostructures spherical particles or lamellar nanostructures. It is noted that the nanoscaled morphologies of the thermosets are quite dependent on the macromolecular topologies of the block copolymers. The separated PS nanophases were arranged into cubic (e.g., bcc, fcc, or simple cubic) lattice in the epoxy thermosets containing the linear PCL-*b*-PS whereas the PS nanophases into lamellar lattice in the thermosets containing the tetra-armed star PCL-*b*-PS. The formation of the morphological difference has been interpreted on the basis of the effects of topological structure of the miscible subchains (i.e., PCL) on the surface free energy of PS nanodomains.

Acknowledgment. Financial support from the Natural Science foundation of China (Project No. 20474038) is acknowl-

edged. S.Z. thanks the Shanghai Educational Development Foundation, China, under an award (2004-SG-18) to the "Shuguang Scholar". This work is also supported by Shanghai Leading Academic Discipline Project (Project No. B202).

References and Notes

(1) Pascault, J. P.; Williams, R. J. J. In *Polymer Blends*; Paul, D. R., Bucknall, C. B., Eds.; Wiley: New York, 2000; Vol. 1, pp 379−415.

(2) (a) Hillmyer, M. A.; Lipic, P. M.; Hajduk, D. A.; Almdal, K.; Bates, F. S. *J. Am. Chem. Soc.* **1997**, *119*, 2749. (b) Lipic, P. M.; Bates, F. S.; Hillmyer, M. A. *J. Am. Chem. Soc.* **1998**, *120*, 8963. (c) Mijovic, J.; Shen, M.; Sy, J. W.; Mondragon, I. *Macromolecules* **2000**, *33*, 5235. (d) Guo, Q.; Thomann, R.; Gronski, W. *Macromolecules* **2002**, *35*, 3133. (e) Guo, Q.; Thomann, R.; Gronski, W. *Macromolecules* **2003**, *36*, 3635. (f) Ritzenthaler, S.; Court, F.; Girard-Reydet, E.; Leibler, L.; Pascault, J. P. *Macromolecules* **2002**, *35*, 6245. (g) Ritzenthaler, S.; Court, F.; Girard-Reydet, E.; Leibler, L.; Pascault, J. P. *Macromolecules* **2003**, *36*, 118. (h) Kosonen, H.; Ruokolainen, J.; Nyholm, P.; Ikkala, O. *Macromolecules* **2001**, *34*, 3046. (i) Grubbs, R B.; Dean, J. M.; Broz, M. E.; Bates, F. S. *Macromolecules* **2000**, *33*, 9522. (j) Rebizant, V.; Abetz, V.; Tournihac, T.; Court, F.; Leibler, L. *Macromolecules* **2003**, *36*, 9889. (k) Dean, J. M.; Verghese, N. E.; Pham, H. Q.; Bates, F. S. *Macromolecules* **2003**, *36*, 9267. (l) Rebizant, V.; Venet, A. S.; Tournillhac, F.; Girard-Reydet, E.; Navarro, C.; Pascault, J. P.; Leibler, L. *Macromolecules* **2004**, *37*, 8017. (m) Dean, J. M.; Grubbs, R. B.; Saad, W.; Cook, R. F.; Bates, F. S. *J. Polym. Sci., Part B: Polym. Phys.* **2003**, *41*, 2444. (o) Wu, J.; Thio, Y. S.; Bates, F. S. *J. Polym. Sci., Part B: Polym. Phys.* **2005**, *43*, 1950. (p) Zucchi, I. A.; Galante, M. J.; Williams, R. J. J. *Polymer* **2005**, *46*, 2603.

(3) (a) Larrañaga, M.; Gabilondo, N.; Kortaberria, G.; Serrano, E.; Remiro, P. M.; Riccardi, C. C.; Mondragon, I. *Polymer* **2005**, *46*, 7082. (b) Meng, F.; Zheng, S.; Zhang, W.; Li, H.; Liang, Q. *Macromolecules* **2006**, *39*, 711. (c) Serrano, E.; Tercjak, A.; Kortaberria, G.; Pomposo, J. A.; Mecerreyes, D.; Zafeiropoulos, N. E.; Stamm, M.; Mondragon, I. *Macromolecules* **2006**, *39*, 2254. (d) Serrano, E.; Larrañaga, M.; Remiro, P. M.; Mondragon, I. *Macromol. Rapid Commun.* **2005**, *26*, 982. (e) Meng, F.; Zheng, S.; Li, H.; Liang, Q.; Liu, T. *Macromolecules* **2006**, *39*, 5072. (f) Meng, F.; Zheng, S.; Liu, T. *Polymer* **2006**, *47*, 7590. (g) Sinturel, C.; Vayer, M.; Erre, R.; Amenitsch, H. *Macromolecules* **2007**, *40*, 2532. (h) Ocando, C.; Serrano, E.; Tercjak, A.; Pena, C.; Kortaberria, G.; Calberg, C.; Grignard, B.; Jerome, R.; Carrasco, P. M.; Mecerreyes, D.; Mondragon, I. *Macromolecules* **2007**, *40*, 4068. (i) Xu, Z.; Zheng, S. *Macromolecules* **2007**, *40*, 2548.

(4) Wang, J.-S.; Matyjaszewski, K. *J. Am. Chem. Soc.* **1995**, *117*, 5614.

(5) Lodge, T. P. *Macromol. Chem. Phys.* **2003**, *204*, 265.

(6) (a) Yin, M.; Zheng, S. *Macromol. Chem. Phys.* **2005**, *206*, 929. (b) Ni, Y.; Zheng, S. *Polymer* **2005**, *46*, 5828.

(7) (a) Dong, C. M.; Qiu, K. Y.; Gu, Z. W.; Feng, X. D. *Macromolecules* **2001**, *34*, 4691. (b) Dong, C. M.; Qiu, K. Y.; Gu, Z. W.; Feng, X. D. *Polymer* **2001**, *42*, 6891. (c) Trollsa, M.; Hedrick, J. L. *J. Am. Chem. Soc.* **1998**, *120*, 4644. (d) Cui, Y.; Ma, X.; Tang, X.; Luo, Y. *Eur. Polym. J.* **2004**, *40*, 299. (e) Núñez, E.; Ferrando, C.; Malmström, E.; Claesson, H.; Werner, P.-E.; Gedde, U. W. *Polymer* **2004**, *45*, 5251. (f) Liu, Y.; Yang, X.; Zhang, W.; Zheng, S. *Polymer* **2006**, *47*, 6814.

(8) (a) Olabisi, O.; Robeson, L. M.; Show, M. T. *Polymer-Polymer Miscibility*; Academic Press, New York, 1979. (b) Utracki, L. A. *Polymer Blends and Alloys*; Hanser Publisher: New York, 1989. (c) Folkes, M. J. Ed. *Polymer Blends and Alloys*; Chapman & Hall: London, 1993.

(9) (a) Fox, T. G. *Bull. Am. Phys. Soc.* **1956**, *1*, 123. (b) Gordon, M.; Taylor, J. S. *J. Appl. Chem.* **1952**, *2*, 496. (c) Couchman, P. R. *Macromolecules* **1978**, *11*, 1156.

(10) (a) Coleman, M. M.; Painter, P. C. *Prog. Polym. Sci.* **1995**, *20*, 1. (b) Coleman, M. M.; Graf, J. F.; Painter, P. C. *Specific Interactions and the Miscibility of Polymer Blends*; Technomic Publishing: Lancaster PA, 1991.

MA7023232